Sputtering yield and secondary electron emission coefficient (γ) of the MgO, $MgAl_2O_4$ and $MgAl_2O_4$/MgO thin film grown on the Cu substrate by using the Focused Ion Beam

Kang-Won Jung*, H. J. Lee, W. H.Jeong, H .J. Oh, E. H. Choi, Y. H. Seo and S. O. Kang
Dept. of Electrophysics, Kwangwoon University, Seoul 139-701, Korea
C. W. Park
Dept. of Mechanical Engineering, Korea Polytechnic University, Gyeonggi-do 429-793
Tel: +82-02-940-5232; E-mail: kang-won@hanmail.net

Abstract

We obtained sputtering yields for the MgO, $MgAl_2O_4$ and $MgAl_2O_4$/MgO films using the FIB system. $MgAl_2O_4$/MgO protective layers have been found to have less 24 ~ 30% sputtering yield values from 0.24 atoms/ion up to 0.36 atoms/ion *than MgO layers with the values from 0.36* atoms/ion *up to 0.45 atoms/ion for irradiated Ga^+ ion beam whose energies ranged from 10 keV to 14 keV. And $MgAl_2O_4$ layers have been found to have lowest sputtering yield values from 0.88 up to 0.11. It is also found that $MgAl_2O_4$/MgO and MgO have secondary electron emission coefficient(γ) values from 0.09 up to 0.12 for Ne^+ ion whose energies ranged from 50 eV to 200 eV.*

1. Introduction

The Focused Ion Beam(FIB) system was developed in early 80's and has been used for various application purposes[1-5]. The liquid metal sources for FIB system are characterized by their high brightness[6] low energy spread and loss rate[7]. Ga, In, Au and Ni are typical liquid ion sources that have been developed for FIB's. The applications of FIB system include maskless ion implantation[8,9], lithography[10,11], micromachining[12], gas evaporation and IC circuit correction and surface analysis. While the ion implantation and lithography require high energies, low energy FIB systems are preferred for high resolution. There exist a bunch of analysis results for the sputtered secondary particles generated from ion beams focused by FIB system. These secondary particles, when injected onto the specimen surface with enough energies, induce various effects, such as sputtering of neutral atoms, emission of positive or negative ions of the substrate material, surface reflection of the injected ions due to collisions with substrate ions or atoms, general radiation in the substrate material, chemical reaction, and growth on the surface layer.

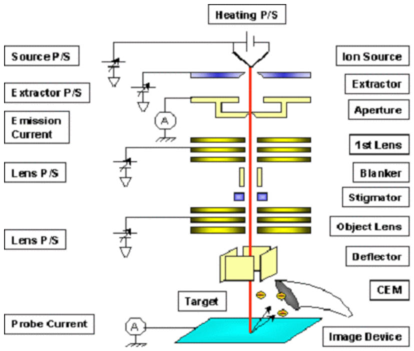

Figure 1. Schematic of FIB system

MgO is chemically unstable especially in humid ambient, it reacts very easily with moisture in the air. In this study, the sputtering and secondary electron emission characteristics MgO, MgAl2O4, and MgAl2O4/MgO dielectric protective have been investigated for AC-PDP (Plasma Display panel). The MgO, $MgAl_2O_4$ layer were grown by 1000 Å thickness and $MgAl_2O_4$/MgO layer were grown by 200/800 Å thickness on the Cu substrate using the electron beam evaporation. An aluminium layer of 1000 Å thickness was overridden on the layer in order to avoid the charging effect of Ga^+ ion beam. We obtained sputtering yield of the MgO, $MgAl_2O_4$ and $MgAl_2O_4$/MgO thin film by using the focused ion beam system. Also, the secondary electron emission coefficient(γ) has been obtained by using the γ-focused ion beam (γ-FIB)[13,14].

2. Experimental configuration

We have measured thickness decrease that allows an estimation of the number of sputtered atoms, and then obtained the net beam current that allowed an estimation of the number of injected ions. Since the probe current is the sum of injected ion current and ejected secondary electron current, from which the incident net ion current Ii can be calculated by subtracting the secondary electron current Is, which is obtained at a collector placed above the specimen, from probe current Ip.

2.1 Measurement of the probe and the secondary particle current

We measured the thickness decrease and estimated the number of atoms in the corresponding sputtered volume, and obtained the ratio of sputtered atoms to the incident ions by calculating the number of ions injected during the sputtered time interval. Fixing the magnification ratio of the digital image, we patterned the sputtered size by patterning program. At the same time, we measured the probe current.

2.2 Estimation of the sputtering yield

The probe currents and the secondary electron currents were measured for different accelerating voltages. The emission current at the ion source was kept at a constant value of 5 μA detected at the Faraday cup, and at the voltage of 1200 V at the channeltron electron multiplier for secondary electron capture. I_p is the probe current, and I_s is the measured current of the secondary electron current. The net beam current is given by ($I_p - |I_s|$). In this way the net beam current was measured for various acceleration voltage. The endpoints refer to the time when the MgO layer begins to be sputtered, and when the sputtered MgO layer reaches copper followed after the all Al are sputtered. Thus, we can detect the endpoint by monitoring variation of the current. The sputtering time duration has been defined by the rising time of either probe or secondary electron current, which is equal to the time interval between the 10 % and 90 % of it.

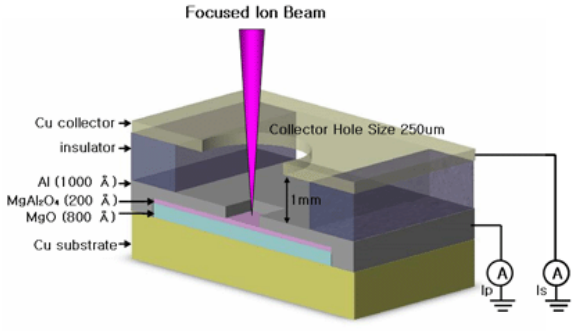

Figure 2. Schematic of the current measurements

Figure 2 shows $MgAl_2O_4/MgO$ layer were grown by 200/800 Å thickness on the Cu substrate using the electron beam evaporation. In order to avoid the charging effect, the Al layer of 1000 Å thickness has been added to top of the MgO layer. The probe current has been measured for the sputtered area of $2.5um \times 2.5um$ in this experiment.

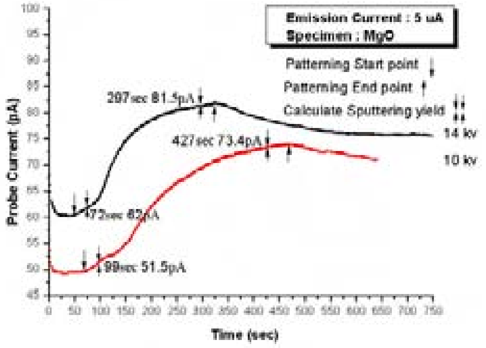

(a) Probe current

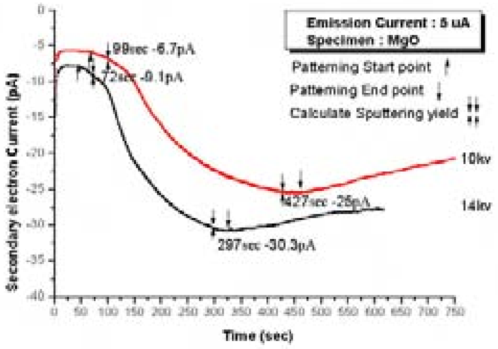

(b) Secondary electron current

Figure 3. Probe (a) and Secondary electron (b) current versus time for MgO for acceleration voltage of 10 kV and 14 kV

Figure 3 shows the probe (a) and secondary electron current (b), respectively, versus time for MgO during the sputtering of specimen by Ga^+ ion beam. The sputtering yield can be estimated by ratio of the number of atoms within the sputtered volume of MgO layer to the number of incident Ga^+ ions. The number of sputtered atoms in the MgO layer can be determined by taking into consideration of the density and volume of the sputtered layer. The density of the MgO layer is 3.58×10^{-12} g/um^3 and the mass of the sputtered MgO is estimated to be 2.24×10^{-12} g. Hence the number of the sputtered MgO atoms is estimated to be 3.34×10^{10} since molecular MgO mass is 6.7×10^{-23} g.

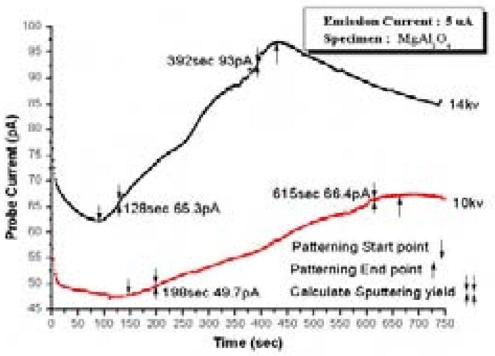

(a)Probe current

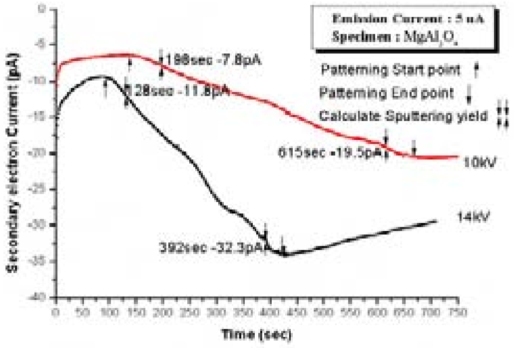

(b) Secondary electron current

Figure 4. Probe (a) and Secondary electron (b) current versus time for $MgAl_2O_4$ for acceleration voltage of 10 kV and 14 kV

Figure 4 shows the probe (a) and secondary electron current (b), respectively, versus time for $MgAl_2O_4$ during the sputtering of specimen by Ga^+ ion beam. The density of the $MgAl_2O_4$ layer is 3.64×10^{-12} g/um^3 and the mass of the sputtered $MgAl_2O_4$ is estimated to be 2.26×10^{-12} g. Hence the number of the sputtered $MgAl_2O_4$ atoms is estimated to be 9.6×10^9 since molecular $MgAl_2O_4$ mass is 2.36×10^{-22} g.

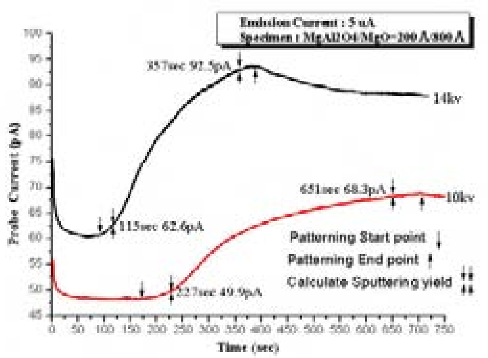

(a)Probe current

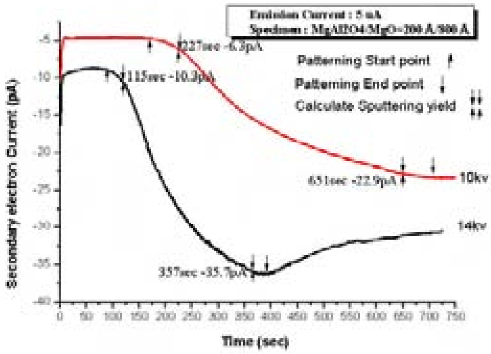

(b)Secondary electron current

Figure 5. Probe (a) and Secondary electron (b) current versus time for $MgAl_2O_4$/MgO for acceleration voltage of 10 kV and 14 kV.

Figure 5 shows the probe (a) and secondary electron current (b), respectively, versus time for the $MgAl_2O_4$//MgO during the sputtering of specimen by Ga^+ ion beam. The mass of the sputtered $MgAl_2O_4$//MgO is estimated to be 2.25×10^{-12} g. Hence the number of the $MgAl_2O_4$/MgO atoms is estimated to be 3.34×10^{10}.

3. Experimental Results

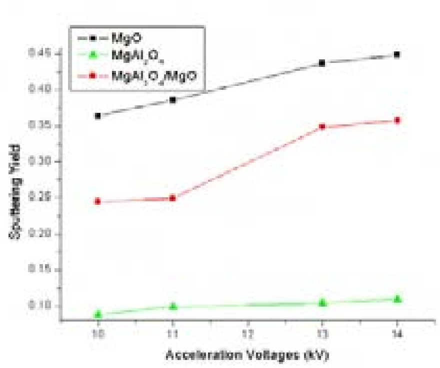

Figure 6. Sputtering yield of MgO, $MgAl_2O_4$, $MgAl_2O_4$/MgO versus ion energy.

Figure 6 shows the sputtering yield for $MgAl_2O_4$/MgO double protective layer, 0.24 atoms/ion and 0.40 atoms/ion, respectively, under 10 keV and 14 keV of Ga+ ion energies. The sputtering yield could be calculated by the ratio of the number of sputtered atoms to that of incident ions for given energy. It is noted that these sputtering yield for the normal MgO protective layer are 0.36 atoms/ion and 0.45 atoms/ion for Ga^+ ion energies of 10 keV ad 14 keV, respectively. The sputtering yield for $MgAl_2O_4$/MgO double protective layer is found to be decreased by 24 % and 30 %, respectively, in comparison with the normal MgO protective layer, for the Ga^+ ion energies of 14 keV and 10 keV.

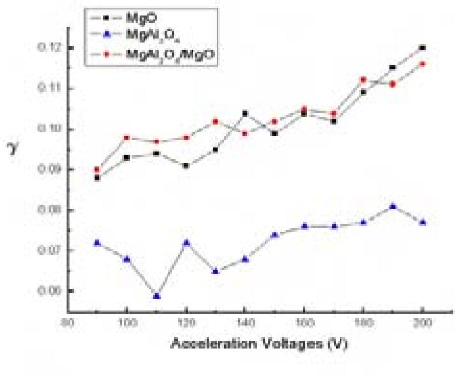

Figure 7. γ of MgO, $MgAl_2O_4$, and $MgAl_2O_4$/MgO films versus Ne^+ ion energy.

Figure 7 shows the secondary electron emission coefficient(γ) of MgO, $MgAl_2O_4$/MgO, $MgAl_2O_4$, and protective layers, represented by the solid squares, solid circles, and solid triangles, respectively, versus Ne^+ ion energies from 90 eV up to 200 eV. The $MgAl_2O_4$/MgO protective layer have been found to have higher γ from 0.09 up to 0.12 than those for $MgAl_2O_4$ films whose are from 0.06 up to 0.07 for Ne^+ ion energies ranged from 90eV to 200 eV. Also it is found that for $MgAl_2O_4$/MgO protective layer of secondary electron emission coefficient(γ) is similar to that for MgO protective layer throughout this experiment.

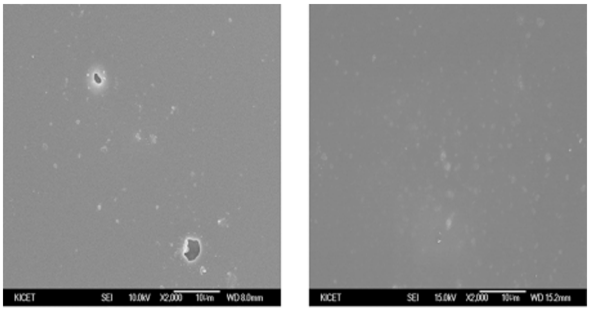

MgO MgAl₂O₄/MgO

Figure 8. SEM micrographs of MgO and $MgAl_2O_4$ /MgO after discharge degradation of 72 Hour.

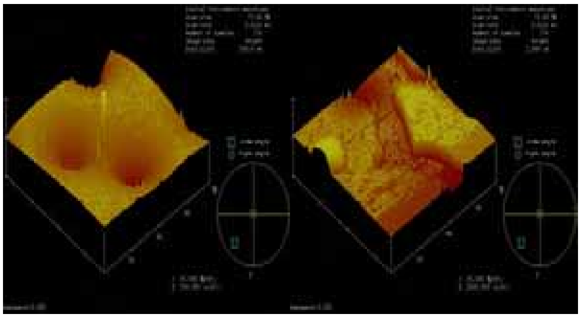

MgO

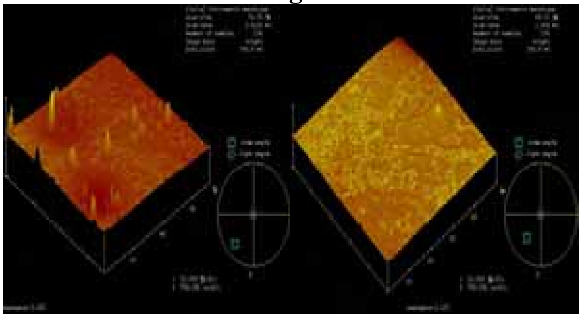

$MgAl_2O_4$/MgO

Figure 9. AFM micrographs of MgO and $MgAl_2O_4$/MgO after discharge degradation of 72 Hour.

Figures 8 and 9 show SEM and AFM images of surface on MgO and $MgAl_2O_4$/MgO protective layer, respectively, after discharge degradation of 72 Hours. It is found that $MgAl_2O_4$/MgO protective layer has superior to MgO protective layer in hardness and discharge degradation in this study.

4. Conclusion

We have measured the sputtering yield and the ion-induced secondary electron emission coefficient(γ) for the MgO, $MgAl_2O_4$ and $MgAl_2O_4$/MgO films. It is found that $MgAl_2O_4$/MgO protective layers has less 24 ~ 30% lower sputtering yield values from 0.24 atoms/ion up to 0.34 atoms/ion than MgO layers with the values of 0.36 atoms/ion up to 0.45 atoms/ion for irradiated Ga^+ ion beam whose energies ranged from 10 keV to 14 keV. It is also concluded that $MgAl_2O_4$/MgO protective layer is recommended as a protective layer for AC-PDP panel life-time, which has similar secondary electron emission coefficient(γ) to the conventional MgO protective layer in alternating plasma display panels.

5. Acknowledgements

This work was partially supported by the next generation new technology project (10011364) from the Ministry of Commerce, and also the 2005 academic research fund from Kwangwon University. The authors gratefully acknowledge this support

6. References

[1] J. Z. Wan, J. G. Simmins and D. A. Thompson, J. Appl. Phys. **81**(2), 765 (1997)

[2] G. Ben Assayag, C. Vieu and J. Gierak, J. Vac. Sci. Technol. B **11**(6), 2420 (1993)

[3] Yeong-Ah Soh, Gregory L. Snider, Michael J. Skvarla and Harold G. Craighead, J. Vac. Sci. Technol. B **11**(6), 2629 (1993)

[4] H. Kim, T. Noda and H. Sakaki, J. Vac. Sci. Technol. B **16**(4), 2547 (1998)

[5] G. Bacher, T. Kümmell, D. Eisert, A Forchel, B. König, W. Ossau, C. R. Becker and G. Landwehr, J. Appl. Phys. **75**, 956 (1999)

[6] L. Seliger, J. W. Ward, V. Wang, and R. L. Kubena, Appl. Phys. Lett. **34**, 310 (1979)

[7] H. S. Uhm, E. H. Choi, G. S. Cho, and S. O. Kang, Phys. Plasmas **1**, 4105 (1994)

[8] M. Tamura, S. Shukuri, M. Moniwa, and M. Default, Appl. Phys. A **39**, 183 (1996)

[9] H. J. Lezec, C. R. Musil, J. Melngailis, L. J. Mahoney, and J. D. Woodhouse, J. Vac. Sci. Technol. B **9**, 2709 (1991)

[10] S. Matsui, Y. Kojima, Y. Ochiai, and Honda, J. Vac. Sci. Technol. B **9**, 622 (1991)

[11] J. S. Huh, M. I. Shepard, and J. Melngailis, J. Vac. Sci. Technol. B **9**, 173, (1991)

[12] T. Ishitani, T. Ohnishi, and Y. Kanwanami, Jpn. J. Appl. Phys. **29**, 2283 (1990)

[13] E. H. Choi, H. J. Oh, Y. G. Kim, J. J. Ko, J. Y. Lim, J, G, Kim, D. I. Kim, G. S. Cho, and S. O. Kang, jpn. J. Appl. Phys., Part 1 **37**, 7015 (1998)

[14] E. H. Choi, J. Y. Lim, Y. G. Kim, J. J. Ko, D. I. Kim, C. W. Lee, and G. S. Cho, J Appl. Phys. **86**, 6525(1999)